

# Microgravity Removes Reaction Limits from Nonpolar Nanoparticle Agglomeration

Andrea Pyttlik, Björn Kuttich, and Tobias Kraus\*

Gravity can affect the agglomeration of nanoparticles by changing convection and sedimentation. The temperature-induced agglomeration of hexadecanethiol-capped gold nanoparticles in microgravity ( $\mu$  g) is studied at the ZARM (Center of Applied Space Technology and Microgravity) drop tower and compared to their agglomeration on the ground (1 g). Nonpolar nanoparticles with a hydrodynamic diameter of 13 nm are dispersed in tetradecane, rapidly cooled from 70 to 10 °C to induce agglomeration, and observed by dynamic light scattering at a time resolution of 1 s. The mean hydrodynamic diameters of the agglomerates formed after 8 s in microgravity are 3 times (for low initial concentrations) to 5 times (at high initial concentrations) larger than on the ground. The observations are consistent with an agglomeration process that is closer to the reaction limit on the ground and closer to the diffusion limit in microgravity.

## 1. Introduction

The crystallization of ions, macromolecules, and particles is known to be affected by gravity through convection, sedimentation, hydraulic and hydrodynamic stresses.<sup>[1,2]</sup> Protein crystals grown in space tend to be larger and show an overall higher quality due to fewer cracks, striations, inclusions, and defects.<sup>[3–6]</sup> It has been suggested that the elimination of convection provides a more uniform environment at the crystal interface that results in a more ordered crystal structure than on the ground.<sup>[7]</sup>

Smith et al. reported increased size and quality of insulin crystals grown during space shuttle flights.<sup>[8]</sup> Littke and John investigated the crystallization of  $\beta$ -galactosidase and lysozyme on the space shuttle mission Spacelab 1 and found larger crystals than on the ground.<sup>[9]</sup> The effect of gravity on the crys-

tallization of hard spheres has been investigated, too. Chaikin et al. dispersed spherical PMMA particles with a diameter of 600 nm in an index-matching mixture of cis-decalin and tetralin as a model system for hard spheres. Observation of the crystallization of these spheres on ground and during a space shuttle mission with time-resolved Bragg light scattering showed that crystals do grow larger and faster in microgravity.<sup>[10]</sup> Günther et al. investigated the formation of agglomerates of nickel nanoparticles via inert gas condensation in the gas phase on ground and during parabolic flights. Chain-like agglomerates were found under normal and microgravity conditions, where the chain length was increased under microgravity con-

ditions.<sup>[11]</sup> Weitz et al. investigated the gelation of polystyrene colloids on the International Space Station (ISS) over 16 days. Larger clusters were formed than on ground, and the authors argued that gravitationally induced stress limits cluster growth and thus, gelation rates.<sup>[12]</sup> Potenza et al. investigated the agglomeration of fluorinated latex nanoparticles on the ISS and reported a different nucleation process than on ground.<sup>[13]</sup>

Little is known about possible effects of gravity on the agglomeration of high-density nanoparticles in dispersion. Metal nanoparticles are important components of systems that may be affected by gravity. Gold nanoparticles are commonly used because they are chemically well-defined, comparatively easy to synthesize, and have interesting optical and electronic properties. They are used as components of nanocomposites,<sup>[14,15]</sup> functional inks,<sup>[16–18]</sup> drug delivery systems,<sup>[19,20]</sup> and biosensors.<sup>[21,22]</sup> The large Hamaker constants of metals lend such nanoparticles strong attractive van der Waals interactions. Agglomeration frequently occurs during material preparation or during the application of nanoparticles in dispersion and affects properties and performance of materials.

Several important applications of gold nanoparticles – from plasmonic assays to the formation of nanocomposites – involve agglomeration. We studied the influence of gravity on the agglomeration of gold nanoparticles capped with alkanethiols in organic solvents. Their interaction can be tuned through the choice of core diameter, shell thickness, and the solvent. Agglomeration can be induced by cooling, as has been shown in detailed previous studies on the particles' interactions.<sup>[23,24]</sup> The solvent type strongly affects the concentration at which agglomeration sets in and the geometry of the agglomerates that form.<sup>[25,26]</sup> We used a high and a low concentration of the particles in the same solvent, induced agglomeration with an

A. Pyttlik, B. Kuttich, T. Kraus  
Structure Formation  
INM Leibniz-Institute for New Materials  
Campus D2 2, 66123 Saarbrücken, Germany  
E-mail: tobias.kraus@leibniz-inm.de

T. Kraus  
Colloid and Interface Chemistry  
Saarland University  
Campus D2 2, 66123 Saarbrücken, Germany

 The ORCID identification number(s) for the author(s) of this article can be found under <https://doi.org/10.1002/smll.202204621>.

© 2022 The Authors. Small published by Wiley-VCH GmbH. This is an open access article under the terms of the Creative Commons Attribution License, which permits use, distribution and reproduction in any medium, provided the original work is properly cited.

DOI: 10.1002/smll.202204621

abrupt temperature drop, and observed the growth via dynamic light scattering (DLS) on ground and in microgravity. Nanoparticles with gold core diameters of 7.8 nm and tetradecane as solvent were chosen as a reliable experimental system with an agglomeration temperature in a suitable range. It is possible to de-agglomerate such dispersions by heating them to 70 °C. Fast agglomeration can be induced by cooling it below 60 °C.

Particle agglomeration was induced under microgravity conditions at the drop tower at the ZARM institute (Center of Applied Space Technology and Microgravity) in Bremen, Germany. The tower has a height of 122 m. A simple drop experiment has a microgravity interval of 4.74 s; the catapult system of ZARM that we used in many experiments extends this to 9.5 s.<sup>[27]</sup> The agglomeration of the gold nanoparticles was observed by following the average hydrodynamic diameter of the dispersion with a series of DLS measurements with 1 s duration using an adapted commercial laser system. DLS is a well-established method to analyze the particle dynamics of colloids from microseconds to seconds. It is often used to reconstruct particle sizes ranging from submicron to a few micrometers from their diffusivity.<sup>[28]</sup> Several DLS experiments have already been performed under microgravity conditions.<sup>[29–32]</sup>

We induced rapid agglomeration of the gold nanoparticles at a well-defined time. The dispersions were kept above their agglomeration temperature and for an extended period to ensure that they were well-dispersed. A defined volume was injected into a precooled measurement cell immediately before the lift-off of the drop tower capsule or the catapult launch. We used previously published results on temperature measurements in the dispersion during microgravity to evaluate the size change due to agglomeration.<sup>[33]</sup>

This manuscript is organized as follows: we first report on the agglomeration of the nanoparticles on ground at two different concentrations and the evolution of their average hydrodynamic diameters. Experiments in microgravity with catapult launches under the same conditions at two concentrations are followed by the results for one concentration in a drop experiment to assess the possible effects of the catapult. We discuss possible mechanisms that accelerate agglomerate growth in microgravity.

## 2. Results and Discussion

Hexadecanethiol-capped gold nanoparticles with an average core diameter of  $d_{\text{Core}} = 7.8 \text{ nm}$  ( $\pm 0.5 \text{ nm}$ , one standard deviation) were chemically synthesized, purified, and dispersed in tetradecane. We studied their dynamic light scattering at different temperatures under normal conditions (1 g) and in microgravity ( $\mu \text{g}$ ). The self-assembled alkylthiol shells of the particles undergo a phase transition at a temperature that depends on core diameter, shell thickness, and solvent.<sup>[23–25,34]</sup> Cooling below this temperature induces rapid agglomeration of particles with small cores, as we have them here.

The deagglomerated particles at 70 °C had a hydrodynamic diameter of  $d_{\text{H}} = 13 \text{ nm}$  ( $\pm 1 \text{ nm}$ ). We quantified the temperature dependence of their agglomeration by small-angle X-ray scattering (SAXS) and DLS measurements as shown in Figure 1. Agglomeration began at 60 °C as indicated by an increased agglomeration fraction  $\chi_{\text{Agglo}}$  and hydrodynamic diameter

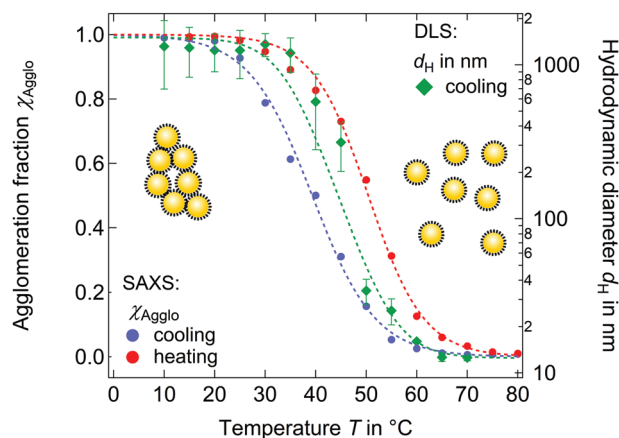


**Figure 1.** Temperature-dependent agglomeration of hexadecanethiol capped gold nanoparticles in tetradecane as indicated by SAXS (left axis) and DLS (right axis). The agglomeration fraction  $\chi_{\text{Agglo}}$  was obtained from SAXS measurements while cooling the sample from 80 to 10 °C and reheating it to 80 °C. The average hydrodynamic diameter  $d_{\text{H}}$  of the growing agglomerates was determined by DLS after cooling the sample from 70 to 10 °C. Each measurement was repeated two times; the means of both measurements and the standard deviations are shown. Dashed lines are sigmoidal curves and serve as guide for the eye.

$d_{\text{H}}$ , see Figure 1. The fraction of agglomerated particles  $\chi_{\text{Agglo}}$  increased with cooling until all particles had agglomerated, as previously described.<sup>[25]</sup>

We studied the agglomeration of rapidly cooled particles in a microgravity-compatible DLS set-up that we describe in detail in an earlier publication.<sup>[33]</sup> Agglomeration was initiated by injecting the hot particle dispersion (70 °C) into the precooled measurement cell (10 °C). We repeated identical experiments on ground and in microgravity multiple times and compared the results. Microgravity was achieved during multiple drops in the ZARM drop tower in Bremen. Their unique catapult system provided a microgravity interval of up to 9.5 s, sufficient time for 8 consecutive DLS measurements with an integration time of 1 s. The autocorrelation function recorded at  $t = 9 \text{ s}$  was affected by the landing of the capsule and the resulting deceleration during impact. The experiments at low particle concentration were repeated three times on ground and twice in the drop tower with a catapult launch; experiments at high particle concentration were repeated twice on ground and four times in the tower with a catapult launch.

### 2.1. Ground Experiment

Agglomeration of gold nanoparticles at a particle concentration of  $c = 1.03 \text{ mg mL}^{-1}$  ( $\pm 0.12 \text{ mg mL}^{-1}$ ) and  $c = 2.75 \text{ mg mL}^{-1}$  ( $\pm 0.04 \text{ mg mL}^{-1}$ ) on ground (1 g) was observed via dynamic light scattering, immediately after the sample injection was completed. Selected autocorrelation functions are shown in the Supporting Information. The set-up reliably recorded autocorrelation functions with an integration time of 1 s.

The temperature inside the scattering volume while cooling the sample from 70 to 10 °C was determined by following an approach developed previously.<sup>[33]</sup> It is based on the temperature-dependent dynamics of nonagglomerating reference particles

that we quantified by dynamic light scattering. These particles are coated with oleylamine that suppresses agglomeration in the entire temperature range and makes them suitable as thermometers.<sup>[33]</sup> The correlation time of their scattering thus solely changes due to the temperature variation inside the scattering volume, allowing for an intrinsic temperature measurement. According to these reference investigations, within the first seconds after sample injection, the temperature in the scattering volume drops below 60 °C, i.e., agglomeration temperature of the samples investigated in this study.<sup>[33]</sup>

We initiated agglomeration on ground and in the drop tower by injecting the temperature-sensitive particles with hexadecanethiol shells so that they were rapidly cooled to below 60 °C. Autocorrelation curves with 1 s measurement time were then continuously recorded from DLS on the agglomerating particle system. Mean residence times  $\tau_{\text{Diff}}$  were obtained from the autocorrelation functions by fitting a single exponential decay, see Equation 1:<sup>[35]</sup>

$$g_2 - 1 = A \cdot \exp\left(-2 \frac{\tau}{\tau_{\text{Diff}}}\right) + c \quad (1)$$

The approach of using a simple mono-exponential decay to an agglomerating system has been introduced by Weitz and others; it neglects the progressing agglomeration and the interaction between the particles but provides reliable estimates on the average agglomerate sizes.<sup>[36,37]</sup> The standard relations, see Equation 2–3:<sup>[32]</sup>

$$q = \frac{4 \cdot \pi \cdot n}{\lambda} \sin(\theta) \quad (2)$$

$$D_{\text{Diff}} = \frac{1}{q^2 \cdot \tau_{\text{Diff}}} \quad (3)$$

and the Stokes-Einstein relation provide the average hydrodynamic diameter  $d_{\text{H}}$ , see Equation 4:<sup>[38]</sup>

$$d_{\text{H}} = \frac{k_{\text{B}} \cdot T}{3 \cdot \pi \cdot \eta \cdot D_{\text{Diff}}} \quad (4)$$

The averaged mean residence times and the corresponding hydrodynamic diameters from three experiments at concentrations of 1.03 mg mL<sup>-1</sup> ( $\pm 0.12$  mg mL<sup>-1</sup>) and two experiments at 2.75 mg mL<sup>-1</sup> ( $\pm 0.04$  mg mL<sup>-1</sup>) are shown in Figure 3. The uncertainties of the mean residence times were obtained from repeated measurements, the uncertainties of the hydrodynamic diameters were estimated based on the uncertainties of temperature measurements that we published previously.<sup>[33]</sup>

The apparent hydrodynamic diameters at  $t = 1$  s were larger than expected and may be affected by the strong convection directly after injection. This is also indicated by the high uncertainty of the diameters that stems mainly from a large uncertainty in the temperature calibration for this first measurement.<sup>[33]</sup> Agglomeration was initially fast and slowed down so that little growth was visible during the remeasurement period as visible in Figure 3. Increasing the initial particle concentration by a factor of 2.7 led to a small increase of agglomerate sizes by a factor of 2 at  $t = 8$  s (Figure 3).

## 2.2. Microgravity Experiments

The experiments were repeated in microgravity ( $\mu$  g) using the same particles at concentrations of 0.86 mg mL<sup>-1</sup> ( $\pm 0.16$  mg mL<sup>-1</sup>) and 3.27 mg mL<sup>-1</sup> ( $\pm 0.79$  mg mL<sup>-1</sup>). Experiments used a microgravity interval of 9.5 s and yielded 8 consecutive autocorrelation functions. The autocorrelation functions at 1 g and in  $\mu$  g shown in Figure 2 illustrate that the measurements are robust and comparable, and that the decay times  $\tau$  were consistently significantly longer in  $\mu$  g. This indicates slower diffusion of the observed agglomerates that can only be caused by larger average hydrodynamic diameters. Interestingly, the single-exponential fit of the autocorrelations from  $\mu$  g was systematically better than of those from 1 g. This is consistent with a wider size distribution of the agglomerates at 1 g than in  $\mu$  g. Samples with broad size distributions lead to broadened autocorrelation functions which deviate from single exponential decay need to be described as a sum of different exponential decays.<sup>[28]</sup>

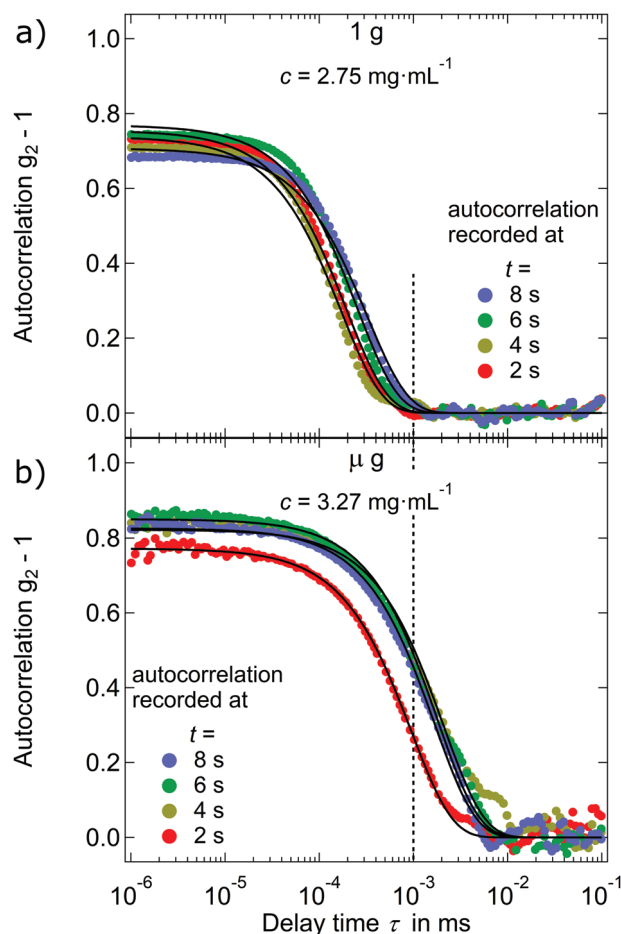


**Figure 2.** Selected autocorrelation functions and exponential fits (black line) of agglomerating hexadecanethiol capped gold nanoparticles in tetradecane at similar concentration on ground 1 g ( $c = 2.75$  mg mL<sup>-1</sup> ( $\pm 0.04$  mg mL<sup>-1</sup>)) and in microgravity  $\mu$  g ( $c = 3.27$  mg mL<sup>-1</sup> ( $\pm 0.79$  mg mL<sup>-1</sup>)). The hot sample (70 °C) was injected into the pre-cooled measurement cell (10 °C) and the autocorrelation functions were recorded after the sample injection was completed.

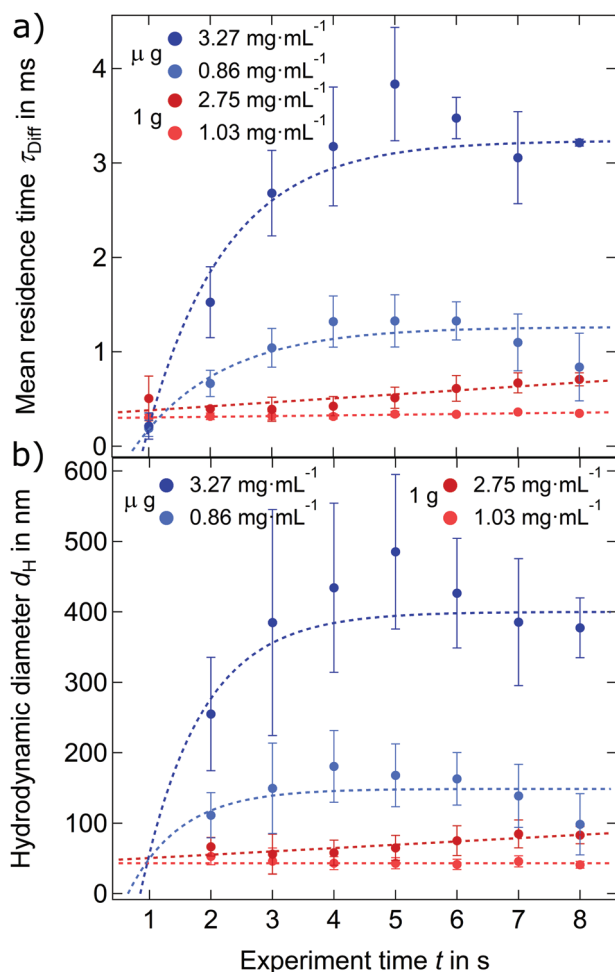


**Figure 3.** a) Mean particle residence times ( $\tau_{Diff}$ ) on ground and in microgravity conditions at different particle concentrations after quenching. The averaged mean residence times of several experiments (see text) and the corresponding standard deviations are shown. b) Apparent hydrodynamic particle diameters  $d_H$ . Average hydrodynamic diameters are shown together with uncertainties estimated using error propagation from the temperature uncertainties (see our previous publication for further information).<sup>[33]</sup> For  $t = 1$  s no hydrodynamic diameters are shown because uncertainties were above 50%. Dashed lines are exponential or linear functions for  $\mu g$  and 1 g, respectively, and serve as guides for the eye.

Average mean residence times  $\tau_{Diff}$  and hydrodynamic diameters  $d_H$  are depicted in **Figure 3**.  $\tau_{Diff}$  was consistently larger in  $\mu g$  than on ground, and it changed more strongly with concentration in  $\mu g$ . Increasing concentration on ground by a factor of 2.7 doubled  $\tau_{Diff}$  after  $t = 8$  s; increasing it in  $\mu g$  by a factor of 3.8 increased  $\tau_{Diff}$  by 3.8, see **Figure 3**. The uncertainties in  $d_H$  were larger for  $\mu g$  than on ground according to error propagation calculations based on the measured standard deviations of  $\tau_{Diff}$  in repeated experiments and the uncertainties of temperature measurements that affect viscosity and refractive index, too. The effects of microgravity on the hydrodynamic diameters of the agglomerates surpass all uncertainties, however, and indicate the growth of larger agglomerates in  $\mu g$ . In the following, we discuss possible mechanisms to explain this difference.

Sedimentation removes agglomerates from the dispersion. It is conceivable that on ground, larger agglomerates form

but cannot be detected, because they settle below the scattering volume of the DLS experiment. However, the agglomerates observed in microgravity are too small to sediment in the time frame of our experiments; at a hydrodynamic diameter of  $d_H = 100$  nm, sedimentation is at least three orders of magnitude slower than the entire experiment (see Supporting Information for the calculation).

More likely is a transition from reaction-limited aggregation (RLA) on ground to diffusion-limited aggregation (DLA) in microgravity. DLA forms agglomerates that are less compact than those from RLA, explaining the observed increase in hydrodynamic diameter. Agglomerate growth rates in RLA depend on the mobility of the particles, their density, and the stiction probability  $p$  of the particles when they collide. Particles collide multiple times before they attach to an agglomerate.<sup>[39]</sup> Dense agglomerates form where each particle is more likely to have multiple neighbors. Such agglomerates may further restructure and age with time to form even denser structures because the particles can still move.<sup>[39,40]</sup>

Ideal DLA requires only one collision to form an agglomerate.<sup>[41]</sup> This leads to open fractals where few particles have more than one immediate neighbor.<sup>[40]</sup> The particles are strongly bound and the agglomerates do not age. Convection and sedimentation prevent this ideal case because they reduce the stiction probability.<sup>[32,41]</sup> Microgravity reduces convection (Rayleigh number  $Ra \approx 0.1$ ) and sedimentation (Archimedes number  $Ar \approx 10^{-14}$ ) and can move RLA-like agglomeration towards a DLA-like process, see **Figure 4** (and SI for calculations).<sup>[32]</sup> Agglomerates formed in DLA show a high fractal dimension of  $D_f = 2.5$  and therefore a higher radius of gyration  $R_G$  for the same number of primary particles. Agglomerates formed in RLA show a much lower fractal dimension; the resulting lower radius of gyration reflects the more compact structure of the agglomerates.<sup>[41]</sup> If all other conditions are similar, DLA is more rapid than RLA, too.<sup>[42–44]</sup> Together, the transition from RLA towards DLA may explain how microgravity led to a more rapid formation of larger agglomerates.

This is consistent with the larger effect of particle concentration in microgravity when we consider that the dispersions are at low volume fractions (between 0.12 vol-% and 0.59 vol-% in our experiments) and that we observe early stages of agglomeration. A larger stiction probability enhances the effect of increased concentrations considerably, while low stiction probability reduces it.

### 3. Conclusion

The effect of gravity on the temperature-induced agglomeration of gold nanoparticles was studied. Microgravity consistently led to the formation of larger agglomerates than under normal conditions. The result was reproducible for different particle concentrations and occurred with or without catapult launches.

The observations can be rationalized when assuming a shift from reaction-limited agglomeration on ground to diffusion-limited agglomeration in microgravity. In microgravity, higher concentrations resulted in the formation of larger agglomerates, as expected for a diffusion-limited process.<sup>[45]</sup>

The microgravity periods available in this study were below 10 s. This report is therefore limited to the initial, rapid stages

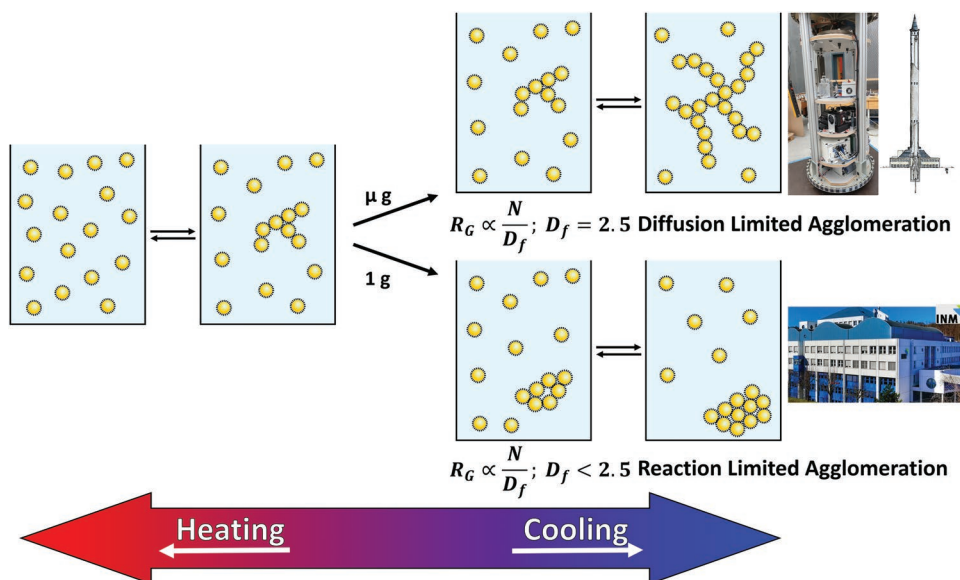


**Figure 4.** Proposed mechanisms for the temperature-induced agglomeration of nonpolar gold nanoparticles on ground (1 g), where agglomeration is more diffusion-limited, and in microgravity ( $\mu$  g), where it is more reaction-limited. Photos reproduced with permission, copyright INM.

of agglomeration. We only observed scattering under a single scattering angle. Additional experiments are planned that will use a sounding rocket to extend the observable time frame and extended optical observation in order to test the hypothesis on the role of gravity that we introduced above.

#### 4. Experimental Section

**Materials and Methods—Synthesis of Gold Nanoparticles:** All chemicals were used without any further purification. Gold nanoparticles stabilized with hexadecanethiol and a core diameter of 7.8 nm were synthesized following the established synthesis protocol of Zheng et al.<sup>[46]</sup> followed by a ligand exchange to remove oleylamine from the gold surface and replaced it with hexadecanethiol, following a modified protocol of Pileni.<sup>[47]</sup> In a mixture of 9 mL benzene (Sigma Aldrich,  $\geq 99\%$ ) and 9 mL oleylamine (Acros Organics, 18 content 80%–90%), 100 mg  $\text{HAuCl}_4 \cdot x\text{H}_2\text{O}$  were dissolved and the solution was flushed with argon. After stirring this mixture for 2.5 min, 40 mg borane *tert*-butylamine (Aldrich, 97 %) dissolved in 1 mL benzene and 1 mL oleylamine were added. The reaction mixture turned from gold-colored to dark red. The reaction mixture was again flushed with argon and stirred for an additional 3 h. The particles were purified by centrifugation after precipitation with a mixture of methanol and ethanol. The particles were washed three times and redispersed in 10 mL of toluene.

For the ligand exchange, the particle dispersion was heated to approximately 100 °C. 1 mL hexadecanethiol was added and the reaction mixture was stirred for 20 min. The particles were again purified by centrifugation after precipitation in a mixture of methanol and ethanol. After the centrifugation, the supernatant was discarded and the particles were redispersed in toluene. The particles were washed three times and finally redispersed in 10 mL tetradecane (ABCR, 99%).

**Particle Characterization:** To determine the core diameter of the gold particles, small angle X-ray measurements were performed using a Xenocs Xeuss 2.0 equipped with a  $K_{\alpha}$  X-ray source ( $\lambda = 0.154$  nm) and a Dectris PILATUS Hybrid Photon Counting Detector. A sample to detector distance of 1200 mm was chosen. To record the 2D diffraction patterns, the integrated FOXTROT v3.4.9 software was used and the data were analyzed with sasfit\_0.94.11.

The gold concentration was measured using ICP-OES (inductive coupled plasma optical emission spectroscopy) with a Horiba

Jobin Yvon Ultima 2 spectrometer at an emission wavelength of 242–795 nm.

**DLS Measurements:** Dynamic light scattering measurements were performed using a customized set-up from LS Instruments (Fribourg, Switzerland), with a laser wavelength of 638 nm, a scattering angle of  $2\theta = 90^\circ$ , and a measurement duration of 1 s. Additional mechanical dumping was added to provide more stability during the catapult launch and the deceleration of the instrument. The measurements were performed with gold concentrations of  $c = 1.03$  mg mL<sup>-1</sup>,  $c = 2.75$  mg mL<sup>-1</sup>,  $c = 0.86$  mg mL<sup>-1</sup>,  $c = 2.67$  mg mL<sup>-1</sup>, or  $c = 3.27$  mg mL<sup>-1</sup> and either under normal gravity (1 g) or under microgravity conditions ( $\mu$  g:  $10^{-6}$  g). The autocorrelation functions were recorded using the 2D pseudo cross mode and analyzed with Origin 2017 (Northampton, United States).

The agglomeration was induced by cooling the sample to below 70 °C. The sample was first heated to 70 °C in an aluminum block for 90–120 min and injected into the precooled measurement cell (10 °C) using a Cetoni syringe pump (Korbussen, Germany) at a flow rate of 3 mL s<sup>-1</sup>.

The agglomeration temperature of the gold nanoparticles was determined by DLS using the Anton Paar Litesizer 500 (Ostfildern-Scharnhausen, Germany). Each measurement was performed with an integration time of 10 s, 30 repetitions, and a scattering angle of 175°. To ensure a stable temperature inside the measurement cell, an equilibration time of 10 min was chosen.

**Microgravity Experiments:** Microgravity conditions of  $10^{-6}$  g were reached during experiments in the drop tower of the ZARM Institute in Bremen. The liquid handling set-up and the DLS instrument were integrated into the drop tower capsule, the capsule was floated with argon and sealed. Catapult launches provided a microgravity interval of 9.1 s, drop experiments a microgravity duration of 4.7 s. The timing of the sample injection was chosen to be finished within the catapult launch or the drop of the capsule and the DLS measurements were triggered at the moment the capsule entered microgravity.

#### Supporting Information

Supporting Information is available from the Wiley Online Library or from the author.

## Acknowledgements

The authors want to thank the German Aerospace Center (DLR, 50WM1763) for funding this research. The microgravity experiments were carried out at the Center of applied Space Technology and Microgravity (ZARM) in Bremen, Germany. The authors want to thank Thorben Könemann and his team from the ZARM Institute for their support by performing the Drop Tower experiments.

Open access funding enabled and organized by Projekt DEAL.

## Conflict of Interest

The authors declare no conflict of interest.

## Data Availability Statement

The data that support the findings of this study are available from the corresponding author upon reasonable request.

## Keywords

diffusion-limited agglomeration, dynamic light scattering, microgravity, nanoparticles, reaction-limited agglomeration

Received: July 27, 2022

Revised: September 19, 2022

Published online: October 10, 2022

- [1] Z. Cheng, P. M. Chaikin, J. Zhu, W. B. Russel, W. V. Meyer, *Phys. Rev. Lett.* **2002**, *88*, 4.
- [2] S. Amselem, *Pharm. Res.* **2019**, *36*, 183.
- [3] A. McPherson, A. J. Malkin, Y. G. Kuznetsov, S. Koszelak, M. Wells, G. Jenkins, J. Howard, G. Lawson, *J. Cryst. Growth* **1999**, *196*, 572.
- [4] B. Lorber, *Biochim. Biophys. Acta, Proteins Proteomics* **2002**, *1599*, 1.
- [5] A. McPherson, L. J. Delucas, *npj Microgravity* **2015**, *1*, 1.
- [6] V. A. Erdmann, C. Lippmann, C. Betzel, Z. Dauter, K. Wilson, R. Hilgenfeld, J. Hoven, A. Liesum, W. Saenger, A. Müller-Fahrnow, W. Hinrichs, M. Düvel, G. E. Schulz, C. W. Müller, H. G. Wittmann, A. Yonath, G. Weber, K. Stegen, A. Plaas-Link, *FEBS Lett.* **1989**, *259*, 194.
- [7] L. J. DeLucas, C. D. Smith, H. W. Smith, S. Vijay-Kumar, S. E. Senadhi, S. E. Ealick, D. C. Carter, R. S. Snyder, P. C. Weber, F. R. Salemme, D. H. Ohlendorf, H. M. Einspahr, L. L. Clancy, M. A. Navia, B. M. McKeever, T. L. Nagabhushan, G. Nelson, A. Mcpherson, S. Koszelak, G. Taylor, D. Stammers, K. Powell, G. Darby, C. E. Bugg, *Science* **1989**, *246*, 651.
- [8] M. M. Long, L. J. DeLucas, C. Smith, M. Carson, K. Moore, R. D. Harrington, D. J. Pillion, S. P. Bishop, W. M. Rosenblum, M. J. Naumann, A. Chait, J. Prah, C. E. Bugg, *Microgravity Sci. Technol.* **1994**, *7*, 196.
- [9] W. Littke, C. John, *Science* **1984**, *225*, 203.
- [10] Z. Cheng, J. Zhu, W. B. Russel, W. V. Meyer, P. M. Chaikin, *Appl. Opt.* **2001**, *40*, 4146.
- [11] S. Lösch, G. N. Iles, B. Schmitz, B. H. Günther, *J. Phys.: Conf. Ser.* **2011**, *327*, 012036.
- [12] S. Manley, L. Cipolletti, V. Trappe, A. E. Bailey, R. J. Christianson, U. Gasser, V. Prasad, P. N. Segre, M. P. Doherty, S. Sankaran, A. L. Jankovsky, B. Shiley, J. Bowen, J. Eggers, C. Kurta, T. Lorik, D. A. Weitz, *Phys. Rev. Lett.* **2004**, *93*, 2.
- [13] M. A. C. Potenza, S. J. Veen, P. Schall, G. H. Wegdam, *EPL* **2018**, *124*, 28002.
- [14] X. Zhao, X. Ding, Z. Deng, Z. Zheng, Y. Peng, X. Long, *Macromol. Rapid Commun.* **2005**, *26*, 1784.
- [15] D. Doblas, J. Hubertus, T. Kister, T. Kraus, *Adv. Mater.* **2018**, *30*, 1.
- [16] D. Huang, F. Liao, S. Molesa, D. Redinger, V. Subramanian, *J. Electrochem. Soc.* **2003**, *150*, G412.
- [17] K. Rajan, I. Roppolo, A. Chiappone, S. Bocchini, D. Perrone, A. Chiolerio, *Nanotechnol. Sci. Appl.* **2016**, *9*, 1.
- [18] S. Jeong, H. C. Song, W. W. Lee, S. S. Lee, Y. Choi, W. Son, E. D. Kim, C. H. Paik, S. H. Oh, B. H. Ryu, *Langmuir* **2011**, *27*, 3144.
- [19] G. R. Bardajee, F. Mizani, S. S. Hosseini, *J. Polym. Res.* **2017**, *24*, 48.
- [20] E. Fazio, A. Scala, S. Grimato, A. Ridolfo, G. Grassi, F. Neri, *J. Mater. Chem. B* **2015**, *3*, 9023.
- [21] M. Srivastava, S. K. Srivastava, N. R. Nirala, R. Prakash, *Anal. Methods* **2014**, *6*, 817.
- [22] Y. Xian, Y. Hu, F. Liu, Y. Xian, H. Wang, L. Jin, *Biosens. Bioelectron.* **2006**, *21*, 1996.
- [23] D. Monego, T. Kister, N. Kirkwood, P. Mulvaney, A. Widmer-Cooper, T. Kraus, *Langmuir* **2018**, *34*, 12982.
- [24] T. Kister, D. Monego, P. Mulvaney, A. Widmer-Cooper, T. Kraus, *ACS Nano* **2018**, *12*, 5969.
- [25] D. Doblas, T. Kister, M. Cano-Bonilla, L. González-García, T. Kraus, *Nano Lett.* **2019**, *19*, 5246.
- [26] D. A. Weitz, J. S. Huang, M. Y. Lin, J. Sung, *Phys. Rev. Lett.* **1984**, *53*, 1657.
- [27] P. von Kampen, U. Kaczmarczik, H. J. Rath, *Acta Astronaut.* **2006**, *59*, 278.
- [28] P. A. Hassan, S. Rana, G. Verma, *Langmuir* **2015**, *31*, 3.
- [29] T. Okubo, A. Tsuchida, K. Kobayashi, A. Kuno, T. Morita, M. Fujishima, Y. Kohno, *Colloid Polym. Sci.* **1999**, *277*, 474.
- [30] R. B. Rogers, W. V. Meyer, J. Zhu, P. M. Chaikin, W. B. Russel, M. Li, W. B. Turner, *Appl. Opt.* **1997**, *36*, 7493.
- [31] D. A. Weitz, A. E. Bailey, S. Manley, V. Prasad, R. Christianson, S. Sankaran, M. P. Doherty, A. L. Jankovsky, T. Lorik, *53rd {International} {Astronautical} {Congress} {International} {Astronautical} {Federation} 2002, IAC-02-J.6*.
- [32] S. Mazzoni, M. A. C. Potenza, M. D. Alaimo, S. J. Veen, M. Dielissen, E. Leussink, J. L. Dewandel, O. Minster, E. Kufner, G. Wegdam, P. Schall, *Rev. Sci. Instrum.* **2013**, *84*, 043704.
- [33] A. Pyttlik, B. Kuttich, T. Kraus, *Microgravity Sci. Technol.* **2022**, *34*, 3.
- [34] P. Born, T. Kraus, *Phys. Rev. E: Stat. Nonlinear, Soft Matter Phys.* **2013**, *87*, 062313.
- [35] J. Gabriel, T. Blochowicz, B. Stühn, *J. Chem. Phys.* **2015**, *142*, 4092.
- [36] M. Y. Lin, H. M. Lindsay, D. A. Weitz, R. C. Ballt, R. Klein, P. Meakin, *Nature* **1989**, *339*, 360.
- [37] D. A. Weitz, M. Y. Lin, C. J. Sandroff, *Surf. Sci.* **1985**, *158*, 147.
- [38] A. Einstein, *Adv. Phys. Res.* **1905**, *322*, 549.
- [39] P. Meakin, *Phys. Rev. A* **1987**, *36*, 5498.
- [40] M. Kolb, R. Jullien, M. Kolb, R. J. Chemically, *J. Phys. Lett.* **1984**, *45*, 977.
- [41] S. J. Veen, O. Antoniuk, B. Weber, M. A. C. Potenza, S. Mazzoni, P. Schall, G. H. Wegdam, *Phys. Rev. Lett.* **2012**, *109*, 1.
- [42] D. A. Weitz, J. S. Huang, *Kinet. Aggregation. Gelation* **1984**, *1984*, 19.
- [43] P. W. J. G. Wijnens, T. P. M. Beelen, C. P. J. Rummens, R. A. van Santen, *J. Non-Cryst. Solids* **1991**, *136*, 119.
- [44] C. Aubert, D. S. Cannell, *Phys. Rev. Lett.* **1986**, *56*, 738.
- [45] M. Lattuada, *J. Phys. Chem. B* **2012**, *116*, 120.
- [46] B. H. Wu, H. Y. Yang, H. Q. Huang, G. X. Chen, N. F. Zheng, *Chin. Chem. Lett.* **2013**, *24*, 457.
- [47] J. Wei, N. Schaeffer, M. P. Pileni, *J. Phys. Chem. B* **2014**, *118*, 14070.